Research Letter

Mex3a protects against atherosclerosis: evidence from mice and humans.

Donato Santovito, M.D. Ph.D.[1,2,3]*, James M. Henderson, Ph.D.[1,2]*, Kiril Bidzhekov, Ph.D.[1]*, Vasiliki Triantafyllidou, M.Sc.[1], Yvonne Jansen, M.Sc.[1], Zhifen Chen, Ph.D.[2,4], Floriana M. Farina, Ph.D.[1,2], Anastasiia Diagel, M.Sc.[4], Maria Aslani, Ph.D.[1], Xavier Blanchet, Ph.D.[1], Heribert Schunkert, M.D.[2,4], Remco T.A. Megens, Ph.D.[1,2,5], Yvonne Döring, Ph.D.[1,2,6], Michael Sattler, Ph.D.[7,8], Christian Weber, M.D.[1,2,9,10,11]

[1]Institute for Cardiovascular Prevention (IPEK), Ludwig-Maximilians-Universität (LMU), Munich, Germany; [2]German Centre for Cardiovascular Research (DZHK), partner site Munich Heart Alliance, Munich, Germany; [3]Institute for Genetic and Biomedical Research (IRGB), Unit of Milan, National Research Council, Milan, Italy; [4]Department of Cardiology, Deutsches Herzzentrum München, Technical University of Munich (TUM), Munich, Germany; [5]Department of Biomedical Engineering, Cardiovascular Research Institute Maastricht (CARIM), Maastricht University, the Netherlands; [6]Division of Angiology, Swiss Cardiovascular Center, Inselspital, University Hospital of Bern, Switzerland; [7]Institute of Structural Biology, Helmholtz Zentrum München, Neuherberg, Germany; [8]Center for Integrated Protein Science Munich at Biomolecular NMR Spectroscopy, Department of Chemistry, Technical University of Munich (TUM), Garching, Germany; [9]Department of Biochemistry, Cardiovascular Research Institute Maastricht (CARIM), Maastricht University, the Netherlands; [10]Cluster for Nucleic Acid Therapeutics Munich (CNATM), Munich, Germany; [11]Munich Cluster for Systems Neurology (SyNergy), Munich, Germany.

* These authors contributed equally.

Correspondence to

Donato Santovito or Christian Weber

Institute for Cardiovascular Prevention (IPEK), Ludwig-Maximilians-University (LMU) of Munich.

Pettenkoferstr. 9, D-80336 München, Germany

Tel.: +49 89 4400 54350; Fax: +49 89 4400 54352

Email: donato.santovito@med.uni-muenchen.de (D.S.); chweber@med.lmu.de (C.W.)

Running title: Mex3a protects against atherosclerosis.

Word count: 800

The RNA-binding protein Mex3a is a component of the processing bodies (P-bodies), establishes RNA-dependent interactions with Argonaute proteins, and is involved in post-transcriptional regulation of gene expression and microRNA function. Besides contributing to neurogenesis and cancer cell stemness[1,2], Mex3a dampens endothelial cell (EC) apoptosis by licensing the biophysical interaction of miR-126-5p with caspase 3 to inhibit its activity.[3] Whereas *Mex3a* deletion in mice increased apoptosis of aortic endothelium[3], its relevance for vascular pathophysiology and atherosclerosis is unknown.

We investigated a mouse model bearing *Mex3a* deletion in an *Apoe*-deficient atherogenic background (*Apoe*$^{-/-}$*Mex3a*$^{-/-}$). The experiments were performed using established protocols[3,4] and approved by local authorities in compliance with institutional guidelines. All supporting data are available within the article or from the corresponding author upon reasonable request. Compared to controls, *Apoe*$^{-/-}$*Mex3a*$^{-/-}$ mice displayed higher permeability to Evans Blue in the aortic vessel wall but not in kidneys, suggesting a role of Mex3a in preserving macro- rather than microvascular integrity (**Figure A**). Evans Blue extravasation did not differ in the brain, arguing against effects on blood-brain barrier permeability. When challenged with a 12-week Western diet, *Apoe*$^{-/-}$*Mex3a*$^{-/-}$ mice developed larger plaques in aortic roots and *en face* prepared aortas (**Figure B,C**), an effect consistent between males and females. Phenotypic characterization of atherosclerotic lesions in the aortic root did not reveal differences in the content of Mac2-positive macrophages or intraplaque fibrosis (stained by Sirius Red), whereas the content of vascular smooth muscle cells (VSMCs, α-smooth muscle actin-positive) was higher in *Apoe*$^{-/-}$*Mex3a*$^{-/-}$ mice (**Figure D**). Plasma cholesterol (**Figure E**) and concentrations of IL-6, IL-9, and TNF-α (**Figure F**) were higher in *Apoe*$^{-/-}$*Mex3a*$^{-/-}$ mice than in controls, possibly reflecting effects on gene expression relevant to lipoprotein metabolism and systemic inflammatory activation, also evidenced by a pro-inflammatory (MHC-II +42.94±0.18%, P=0.028; CD301 -27.78±0.08%, P=0.014) flow cytometric profile of lesional macrophages. Together, our data indicate an atheroprotective role of Mex3a in mice that extends beyond preserving arterial endothelial integrity to potential effects on VSMC abundance and phenotype, endothelial-to-mesenchymal transition, lipid metabolism, and inflammation.

To examine translational relevance for humans, we screened a metanalysis of genome-wide association studies including 210,842 coronary artery disease (CAD) cases among 1,378,170 participants.[5] The *MEX3A* locus was associated with CAD at a significance level approximating a 1% false discovery rate (**Figure G,H**). To gain insights into directionality, we explored genetically regulated *MEX3A* expression using skin-derived expression quantitative trait loci (eQTL) from the Genotype-Tissue Expression (GTEx) database, as the high sample size and *MEX3A* expression in this tissue strengthened statistical power. The CAD risk allele (A) of both lead (rs11264432) and linkage disequilibrium variants (rs10047112) associated with lower *MEX3A* expression (normalized effect size, NES -0.237, P=7.8x10^{-10} and NES -0.292, P=1.9x10^{-15}, respectively). While eQTLs of arterial vessels did not yield significant associations (likely biased by low *MEX3A* reads in bulk sequencing), a weak signal was found for rs10047112(A) in the aorta (NES -0.101, P=0.04). Likewise, *MEX3A* expression was lower in the aorta of CAD patients, as compared to controls (q=7.8x10^{-3}) in the Stockholm-Tartu Atherosclerosis Reverse Networks Engineering Task (STARNET) cohort, reinforcing the notion that lower *MEX3A* expression associates with CAD. In line, rare predicted loss-of-function (pLoF)

MEX3A variants in the UK Biobank exome-sequence data associated with 158 out of 3579 traits tested with the Genebass browser for a nominal $P<0.05$ (by Sequence Kernel Association Test, SKAT-O). Besides cystatin C ($\beta=0.040$, $P=1.4\times10^{-4}$), these included plasma C-reactive protein ($\beta=0.031$, $P=8.1\times10^{-3}$) and total fatty acids ($\beta=0.027$, $P=5.7\times10^{-3}$), as well as atherosclerosis-associated clinical outcomes, e.g., "cerebral infarction" (odds ratio, OR 1.134, $P=0.022$) and "vascular/heart problems diagnosed by doctor" (OR 1.098, $P=0.039$), thus emulating our results in mice.

Finally, we aimed to identify the cellular source of MEX3A in human atherosclerosis. In a single-cell transcriptome dataset of human carotid atherosclerotic plaques (GSE159677, n=51,981 cells), *MEX3A* showed the highest expression in EC clusters in the Uniform Manifold Approximation and Projection (UMAP) but rather moderate expression in VSMCs, macrophages, NK and T cells (**Figure I**). While *MEX3A* did not define a specific EC cluster, it was primarily expressed in arterial ECs positive for *PECAM1*, *GJA4*, and *GJA5* rather than those positive for *ACKR1* or *RGCC*, indicating its relevance in the macro- *vs.* microvascular environment. Differential gene analysis of MEX3A-positive *vs.* MEX3A-negative ECs revealed changes in transcripts involved in vascular development and morphogenesis (**Figure J,K**), further supporting a role of MEX3A in processes of arterial integrity.

In conclusion, we combined data from transgenic mice with genetic association analyses in large cohorts of CAD patients to reveal a protective function of Mex3a in atherosclerosis across mice and humans. While beneficial effects safeguarding endothelial integrity are likely an underlying mechanism, MEX3A expression beyond vascular endothelium (e.g., liver, adipose tissue) and our results on inflammatory biomarkers and lipid metabolism imply a broader role in vascular health. Future research using conditional deletion models should dissect such cell-specific contributions in vascular biology. Yet, our study unequivocally establishes that Mex3a serves as an important vasoprotective player with possible therapeutic implications.

Acknowledgments

C.W. is van der Laar-Professor of Atherosclerosis.

Funding Sources

This work was supported by the Deutsche Forschungsgemeinschaft (DFG) SFB1123-A1/A10 to Y.D. and C.W, SFB1123-Z1 to R.T.A.M, SFB1123-B5 to D.S., 403584255 - TRR 267-A2 to C.W. and M.S., TRR 267-B5 to Z.C. and H.S., by the German Centre for Cardiovascular Research (DZHK) 81Z0600202 to C.W., and 81Z0600203 and 81X2600269 to D.S.; by LMUexcellent, funded by the Federal Ministry of Education and Research (BMBF) and the Free State of Bavaria under the Excellence Strategy of the Federal Government and the Länder to D.S., and by the BMBF in the framework of the Cluster4Future program (Cluster for Nucleic Acid Therapeutics Munich, CNATM) to M.S. and C.W.

Conflict of Interest Disclosures

None.

References

1. Álvarez-Varela A, Novellasdemunt L, Barriga FM, Hernando-Momblona X, Cañellas-Socias A, Cano-Crespo S, Sevillano M, Cortina C, Stork D, Morral C, *et al.* Mex3a marks drug-tolerant persister colorectal cancer cells that mediate relapse after chemotherapy. *Nat Cancer.* 2022;3:1052–1070.
2. Domingo-Muelas A, Duart-Abadia P, Morante-Redolat JM, Jordán-Pla A, Belenguer G, Fabra-Beser J, Paniagua-Herranz L, Pérez-Villalba A, Álvarez-Varela A, Barriga FM, *et al.* Post-transcriptional control of a stemness signature by RNA-binding protein MEX3A regulates murine adult neurogenesis. *Nat Commun.* 2023;14:373.
3. Santovito D, Egea V, Bidzhekov K, Natarelli L, Mourão A, Blanchet X, Wichapong K, Aslani M, Brunßen C, Horckmans M, *et al.* Noncanonical inhibition of caspase-3 by a nuclear microRNA confers endothelial protection by autophagy in atherosclerosis. *Sci Transl Med.* 2020;12:eaaz2294.
4. Cimen I, Natarelli L, Kichi ZA, Henderson JM, Farina FM, Briem E, Aslani M, Megens RTA, Jansen Y, Mann-Fallenbuchel E, *et al.* Targeting a cell-specific microRNA repressor of CXCR4 ameliorates atherosclerosis in mice. *Sci Transl Med.* 2023;15:eadf3357.
5. Aragam KG, Jiang T, Goel A, Kanoni S, Wolford BN, Atri DS, Weeks EM, Wang M, Hindy G, Zhou W, *et al.* Discovery and systematic characterization of risk variants and genes for coronary artery disease in over a million participants. *Nat Genet.* 2022;54:1803–1815.

Nonstandard Abbreviations and Acronyms

αSMA, alpha-smooth muscle actin

CAD, coronary artery disease

EC, endothelial cells

eQTL, expression quantitative trait loci

FDR, false discovery rate

GTEx, genotype-tissue expression

NES, normalized effect size

OR, odds ratio

pLOF, predicted loss-of-function

SKAT-O, sequence kernel association test O

STARNET, Stockholm-Tartu atherosclerosis reverse networks engineering task

UMAP, uniform manifold approximation and projection

VSMC, vascular smooth muscle cell

Figure Legend

MEX3A deletion exacerbates atherosclerosis in mice and variants in the *MEX3A* locus associate with CAD in humans. A, Representative images of aortic arches, and spectrophotometric quantification of Evans blue extravasation in aortas, kidneys and brains of control *Apoe*$^{-/-}$ and *Apoe*$^{-/-}$*Mex3a*$^{-/-}$ mice one hour after intravenous injection of Evans blue (n=8-11 animals). Scale bar, 1 mm. **B**, Representative Elastic van Gieson (EvG) staining and quantification of atherosclerotic lesion size in aortic roots of *Apoe*$^{-/-}$ and *Apoe*$^{-/-}$*Mex3a*$^{-/-}$ mice fed a Western diet (21% crude fat, 0.15% cholesterol, 19.5% protein, Western-style diet food TD.88137, ssniff) for 12 weeks (n=11 animals). **C**, Representative Oil-Red-O staining, and quantification of lesion area in *en face* prepared aortas of *Apoe*$^{-/-}$ and *Apoe*$^{-/-}$*Mex3a*$^{-/-}$ mice fed a Western diet for 12 weeks (n=6 animals). **D**, Representative immunofluorescent staining for Mac2 (clone M3/38, Cedarlanelabs, Cat# CL8942AP), α-smooth muscle actin (αSMA, clone 1A4, Sigma Aldrich Cat# F3777), and Hoechst to counterstain cell nuclei and quantification of the lesional content of Mac2-positive macrophages, αSMA-positive VSMCs, and intraplaque fibrosis (Sirius Red Staining) (n=7-11 animals). Scale bar, 100 µm. **E**, Plasma cholesterol concentration in *Apoe*$^{-/-}$ and *Apoe*$^{-/-}$*Mex3a*$^{-/-}$ mice fed a Western diet for 12 weeks, as quantified by enzymatic assays (c.f.a.s. cobas, Roche Diagnostics) (n=11 animals). **F**, Heatmap of mean ranks of inflammatory cytokines in plasma of *Apoe*$^{-/-}$ and *Apoe*$^{-/-}$*Mex3a*$^{-/-}$ mice as assessed by multiplexed immunoassays (ProcartaPlex EPX010-20440-901, ThermoFisher Scientific). Statistically significant differences for a false discovery rate (FDR) <5% are given. **G**, Regional association plot of the *MEX3A* locus (chr1:156.029.000-156.061.000) based on the summary statistics of the Coronary Artery Disease Genome-Wide Replication and Metanalysis (CARDIoGRAMplusC4D) consortium (1,378,170 individuals).[5] Dots indicate the genomic position in GRCh37 coordinates (x-axis) and the -$\log_{10}$(meta-analysis *P* value) (y-axis) of each variant. Colored dots mark rs11264432, the lead variant, and rs10047112, the variant in linkage disequilibrium (R^2=0.452, D'=0.760). The dashed line delineates the threshold for statistical significance approximating an FDR <1% (P<2.5x10^{-5}) calculated using the "*q* value" R package to consider all the variants in the genome-wide analysis, as detailed in the derivative meta-analysis.[5] **H**, Forest plot showing odds ratios and 95% confidence intervals for CAD association of rs11264432 and rs10047112 in Aragam *et al.*[5] **I**, Expression pattern of *MEX3A* in individual cell clusters visualized using Uniform Manifold Approximation and Projection (UMAP) in a dataset of human atherosclerotic plaques (GSE159677). Cells were excluded based on the number of genes (<200 or >4000) and percentage of mitochondrial transcripts (>10%), the 45,826 retained cells were down-sampled to account for an equal cell number across patients in the final dataset (13,267 cells). The dot plot shows the average expression and proportion of cells expressing *MEX3A* in the individual cell clusters in UMAP. Zero-preserving data imputation (ALRA) was applied. **J**, Heatmap showing differentially expressed genes ($\log_2$FC >|0.2|, FDR<10%) in ECs positive (MEX3A$^+$) or negative (MEX3A$^-$) for *MEX3A* expression in human atherosclerotic plaques. MEX3A$^+$ cells were defined by an expression >0.5 upon ALRA. Data were analyzed using DESeq2 on pseudobulk expression profiles for each individual created using the AggregateExpression function in Seurat and depicted as *z* scores in the heatmap. **K**, Gene ontology analysis for the differentially expressed genes in **J**. *P* values for enrichment were computed with a hypergeometric test and corrected (i.e.,

145 *q* values) for multiple comparisons with the Benjamini–Hochberg procedure using MetaScape. The graph
146 depicts enriched terms for $q<0.05$ (i.e., GO:0001568, 0001525, 0001944, 0048514, 0035239), the dashed line
147 delineates the threshold for statistical significance ($q<0.05$), and the dot size reflects the proportion of gene
148 overlapping in each term. For the atherosclerosis experiments, *a priori* calculation of power based on previous
149 data in literature and pilot experiments was performed that aimed at 80% statistical power for detecting
150 biological relevant changes (50%) with a two-tailed α-value of 0.05. No randomization was performed due to
151 the case-control study design. Quantification was performed in a blinded manner. Animals were excluded from
152 analyses only in the presence of severe health issues, samples were excluded in case of technical issues during
153 processing. For all experiments, male and female mice were combined in similar proportions. Data in **A-F** are
154 shown as mean and s.e.m. and analyzed using Prism v.10.2 (GraphPad Inc.) by non-parametric Mann-Whitney
155 *U* test, to avoid assumptions on data distribution. Results in **F** were corrected for FDR with the step-up
156 Benjamini-Hochberg approach. A 2-tailed *P* value <0.05 was deemed as statistically significant.

Monocyte subsets in cardiovascular disease: a biomarker perspective

Michael Hristov[1], Christian Weber[1,2]

[1]Institut für Prophylaxe und Epidemiologie der Kreislaufkrankheiten (IPEK), Ludwig-Maximilians-Universität (LMU), München, Germany

[2]Deutsches Zentrum für Herz-Kreislauf-Forschung (DZHK), München, Germany

Correspondence to:
Christian Weber, MD
Institut für Prophylaxe und Epidemiologie der Kreislaufkrankheiten (IPEK)
LMU München
Pettenkoferstr. 9, DE-80336 München
Phone: +49-(0)89-5160-4350
Fax: +49-(0)89-5160-4352
Email: christian.weber@med.uni-muenchen.de

Summary

Endothelial dysfunction together with a dysregulated immune response and lipid accumulation are important confounding factors in the onset and chronic development of atherosclerosis. Recently, a large body of data has emerged on the sequential involvement of different immune cell types, including monocytes, in the pathology of this disease.[1] In this condensed review, we aim to highlight some of the recent basic research and clinical findings on monocyte subsets published since our joint ESC consensus document[2], and reevaluate their potential relevance as surrogate biomarkers in coronary artery disease (CAD).

Monocyte biology

Monocytes are the largest blood leukocytes in adults and have a rapid turnover with relatively short lifespan of only a few days in the bloodstream. As cells of innate immunity they are released from the bone marrow and serve as precursors to tissue macrophages and dendritic cells. Monocytes can secrete inflammatory cytokines and have distinct surface receptors such as integrins, G-protein-coupled and Toll-like receptors (TLRs) that allow adhesion, crawling and migration, as well as direct immune response and phagocytosis.[3-6] In addition to resolving inflammation, monocytes are involved in angiogenesis, tissue remodeling after injury or scavenging apoptotic cells and toxic debris at homeostatic conditions.[3-6]

Monocyte heterogeneity: phenotype and function

According to the expression intensity of the lipopolysaccharide (LPS) receptor CD14 and the FcγIII receptor CD16, human monocytes have typically been divided into three major subsets: classical $CD14^{++}CD16^{-}$, intermediate $CD14^{++}CD16^{+}$ and nonclassical $CD14^{+}CD16^{++}$.[7] These subsets differ significantly in phenotype and function.

The $CD14^{++}CD16^{-}$ subset (~85% of total monocytes) highly expresses Ccr2, Cxcr4, FcγRI, L-selectin and scavenger receptor class A.[5,8-10] In contrast, $CD14^{+}CD16^{++}$ monocytes (~10%) are smaller and less dense showing higher levels of SLAN, CD31, CD11c and Cx3cr1 but much lower levels of Ccr2 compared to the classical subset.[5,8-10] The $CD14^{++}CD16^{+}$ subset (~5%) can be clearly distinguished from the nonclassical by the expression of Ccr2.[10] This lowest subset is strong pro-inflammatory with some unique features that distinguish it from the other two. So far, $CD14^{++}CD16^{+}$ monocytes are enriched in bone marrow and have highest expression of angiogenic markers, CD163, MHC class II, HLA-DR and miR-6087of any subset.[5,8-11] Recent comprehensive data obtained by modern technology like mass cytometry with clustering algorithm and RNA sequencing suggest even higher heterogeneity among each subset with 3 newly identified nonclassical and 4 classical monocytes.[12]

Functionally, classical monocytes are professional phagocytes that generate reactive oxygen species (ROS) and secrete cytokines upon LPS stimulation.[5] In contrast, nonclassical monocytes do not generate ROS and are weak phagocytes that preferentially take up oxidized LDL (ox-LDL), but secrete substantial amounts of inflammatory cytokines after TLR-dependent activation by viruses and nucleic acids.[5,6] Thus, nonclassical monocytes may serve as patrolling immune cells that selectively remove virally infected or injured cells and detoxify ox-LDL. The lower phagocytic activity of $CD14^{+}CD16^{++}$ compared to classical monocytes has been efficiently exploited to enumerate the number and ratio of both subsets

by their differential uptake of magnetic nanoparticles.[13] Finally, the intermediate subset does not produce ROS, but shows the highest secretion of TNF-α and IL-1β in response to LPS.[6]

Monocyte subsets undergo linear maturation kinetics in the periphery that is accompanied by gradual increase in the expression of specific miRNAs.[11] Isotope labelling has revealed that they enter the bloodstream as classical, leave it as intermediate and re-enter as nonclassical.[14] In contrast to the circulation, we found that the intermediate subset was highly enriched in the bone marrow.[15] This medullar monocyte pool seems to require Ccr2, Cxcr4 and possibly CD44 for mobilization and may give rise to more specialized peripheral $Ccr2^{+}$ classical monocytes with implication during inflammation and infection whereas nonclassical monocytes are less abundant in the bone marrow.

Monocyte subsets in CAD: risk prediction and treatment

Epidemiological data twenty years ago have described leukocytosis as an independent risk factor and predictor of future cardiovascular events.[16] Monocyte counts were also positively correlated with in-stent restenosis.[17] Sequential analysis of monocytes by flow cytometry over the last decade has further refined this knowledge and allowed a more detailed assessment of the prognostic value of each subset.

Recently published data has shown that intermediate and nonclassical monocytes predict major adverse cardiovascular events and poor outcome in patients with ST-elevation myocardial infarction (STEMI).[18-20] Intermediate monocyte activation, as assessed by CD11c expression, was also positively correlated with peak levels of troponin and creatin kinase in patients with MI.[21] Beyond MI, $CD14^{++}CD16^{+}$ monocyte counts were associated with coronary plaque vulnerability in a prospective study of patients with CAD.[22] The intermediate subset further predicts severe coronary stenosis in asymptomatic individuals as shown in another retrospective study.[23] Another study revealed a persistent increase in this subset after elective percutaneous coronary intervention (PCI) as part of the residual inflammation.[24]

Collectively, these data are consistent with the first prospective, large cohort study showing that intermediate monocytes are independent predictors of cardiovascular events in risk patients undergoing elective coronary angiography.[25] Furthermore, intermediate and nonclassical monocytes were positively correlated to CAD severity and older participants without manifested chronic disease but with high cardiometabolic risk had elevated percentages of only nonclassical monocytes.[26,27]

In patients with stable CAD on statin treatment high levels of PCSK9 associated with increased classical but decreased nonclassical monocytes while the intermediate subset did not differ.[28] The effects of statins on monocyte subsets are elusive and a prospective randomized trial is still missing. In diseases other than CAD, treatment with prednisolone in patients with immune thrombocytopenia reduced the number of intermediate monocytes and attenuated their pro-inflammatory phenotype.[29] Beta blockers also blunted the mobilization of nonclassical monocytes after acute exercise in healthy cyclist.[30] Further data in healthy donors have shown that classical monocytes generate more angiotensin and express higher levels of both, angiotensin-converting enzyme type 1 (ACE1) and ACE2 than the other subsets.[31]

Finally, in healthy human volunteers under LPS-induced low-grade inflammation, intermediate and nonclassical monocytes showed the highest inflammatory response by their expression of IL-6 and IL-8.[32] Given the role of IL-6 and IL-8 in the pathogenesis of cardiovascular disease, this may have implications for risk prediction and potential new treatment options.

Concluding remarks

Differential monitoring, especially of intermediate monocyte counts, appears to predict cardiovascular events and may also be of interest in identifying individuals with subclinical atherosclerosis. In addition, subset-tailored drug targeting could lead to the development of novel and more specific therapeutics. The effects of approved drugs such as glucocorticoids, statins, PCSK9- or ACE-inhibitors and beta blockers could also be re-evaluated in relation to monocyte subsets.

It is still essential to define reference values for monocyte subsets in the general population by means of a standardized flow cytometry protocol. Meanwhile, the common markers such as CD14, CD16, HLA-DR and Ccr2 are available as dried, pre-aliquoted multicolor antibody cocktail and could be used routinely on simple flow cytometers equipped with two lasers. There is also consensus on the gating strategy and the enumeration of absolute counts for each subset.[2] However, the above reagents are currently licensed for research use only. It is therefore important to work towards having them certified for clinical diagnostic use. While standard instrument equipment and easy-to-use protocols are more useful for clinical routine, expensive, high-performance technology with enhanced resolution, such as multiparameter flow cytometry or even mass cytometry, seems essential and more appropriate for basic research.

Taken together, a comprehensive approach could integrate monocyte subsets, alone or in multiple panels, as novel reliable predictive and diagnostic biomarkers, but also as selective therapeutic targets in cardiovascular precision medicine.

Acknowledgements

The authors are supported by the Deutsche Forschungsgemeinschaft (SFB 1123) and the August-Lenz-Stiftung.

References

1. Weber C, Noels H. Atherosclerosis: current pathogenesis and therapeutic options. Nat Med 2011;17:1410-22.
2. Weber C, Shantsila E, Hristov M, et al. Role and analysis of monocyte subsets in cardiovascular disease. Joint consensus document of the European Society of Cardiology (ESC) Working Groups "Atherosclerosis & Vascular Biology" and "Thrombosis". Thromb Haemost 2016;116:626-37.
3. Auffray C, Sieweke MH, Geissmann F. Blood monocytes: development, heterogeneity, and relationship with dendritic cells. Annu Rev Immunol 2009;27:669-92.
4. Shi C, Pamer EG. Monocyte recruitment during infection and inflammation. Nat Rev Immunol 2011;11:762-74.
5. Ruder AV, Wetzels SMW, Temmerman L, Biessen EAL, Goossens P. Monocyte heterogeneity in cardiovascular disease. Cardiovasc Res 2023;119:2033-2045.
6. Cros J, Cagnard N, Woollard K, et al. Human CD14dim monocytes patrol and sense nucleic acids and viruses via TLR7 and TLR8 receptors. Immunity 2010;33:375-86.
7. Ziegler-Heitbrock L, Ancuta P, Crowe S, et al. Nomenclature of monocytes and dendritic cells in blood. Blood 2010;116:e74-80.
8. Wong KL, Tai JJ, Wong WC, et al. Gene expression profiling reveals the defining features of the classical, intermediate, and nonclassical human monocyte subsets. Blood 2011;118:e16-31.
9. Zawada AM, Rogacev KS, Rotter B, et al. SuperSAGE evidence for CD14++CD16+ monocytes as a third monocyte subset. Blood 2011;118:e50-e61.
10. Shantsila E, Wrigley B, Tapp L, et al. Immunophenotypic characterization of human monocyte subsets: possible implications for cardiovascular disease pathophysiology. J Thromb Haemost 2011;9:1056-66.
11. Zawada AM, Zhang L, Emrich IE, et al. MicroRNA profiling of human intermediate monocytes. Immunobiology 2017;222:587-596.
12. Hamers AAJ, Dinh HQ, Thomas GD, et al. Human monocyte heterogeneity as revealed by high-dimensional mass cytometry. Arterioscler Thromb Vasc Biol 2019;39:25-36.
13. Wildgruber M, Lee H, Chudnovskiy A, et al. Monocyte subset dynamics in human atherosclerosis can be profiled with magnetic nano-sensors. PLoS One 2009;4: e5663.
14. Tak T, Drylewicz J, Conemans L, et al. Circulatory and maturation kinetics of human monocyte subsets in vivo. Blood 2017;130:1474-1477.
15. Mandl M, Schmitz S, Weber C, Hristov M. Characterization of the CD14++CD16+ monocyte population in human bone marrow. PLoS One 2014;9:e112140.
16. Madjid M, Awan I, Willerson JT, et al. Leukocyte count and coronary heart disease: implications for risk assessment. J Am Coll Cardiol 2004;44:1945-56.
17. Fukuda D, Shimada K, Tanaka A, Kawarabayashi T, Yoshiyama M, Yoshikawa J. Circulating monocytes and in-stent neointima after coronary stent implantation. J Am Coll Cardiol 2004;43:18-23.
18. Shantsila E, Ghattas A, Griffiths HR, Lip GYH. Mon2 predicts poor outcome in ST-elevation myocardial infarction. J Intern Med 2019;285:301-316.
19. Abo-Aly M, Shokri E, Chelvarajan L, Tarhuni WM, Tripathi H, Abdel-Latif A. Prognostic significance of activated monocytes in patients with ST-elevation myocardial infarction. Int J Mol Sci 2023;24:11342.

20. Boidin M, Lip GYH, Shantsila A, Thijssen D, Shantsila E. Dynamic changes of monocytes subsets predict major adverse cardiovascular events and left ventricular function after STEMI. Sci Rep 2023;13:48.
21. Foster GA, Gower RM, Stanhope KL, Havel PJ, Simon SI, Armstrong EJ. On-chip phenotypic analysis of inflammatory monocytes in atherogenesis and myocardial infarction. Proc Natl Acad Sci U S A 2013;110:13944-9.
22. Yamamoto H, Yoshida N, Shinke T, et al. Impact of CD14(++)CD16(+) monocytes on coronary plaque vulnerability assessed by optical coherence tomography in coronary artery disease patients. Atherosclerosis 2018 ;269:245-251.
23. Lo SC, Lee WJ, Chen CY, Lee BC. Intermediate CD14++CD16+ monocyte predicts severe coronary stenosis and extensive plaque involvement in asymptomatic individuals. Int J Cardiovasc Imaging 2017;33:1223-1236.
24. Merinopoulos I, Bhalraam U, Holmes T, et al. Circulating intermediate monocytes CD14++CD16+ are increased after elective percutaneous coronary intervention. PLoS One 2023;18:e0294746.
25. Rogacev KS, Cremers B, Zawada AM, et al. CD14++CD16+ monocytes independently predict cardiovascular events: a cohort study of 951 patients referred for elective coronary angiography. J Am Coll Cardiol 2012;60:1512-20.
26. Arnold KA, Blair JE, Paul JD, Shah AP, Nathan S, Alenghat FJ. Monocyte and macrophage subtypes as paired cell biomarkers for coronary artery disease. Exp Physiol 2019;104:1343-1352.
27. Markofski MM, Flynn MG. Elevated circulating CD16+ monocytes and TLR4+ monocytes in older adults with multiple cardiometabolic disease risk factors. Exp Gerontol 2021;154:111530.
28. Krychtiuk KA, Lenz M, Hohensinner P, et al. Circulating levels of proprotein convertase subtilisin/kexin type 9 (PCSK9) are associated with monocyte subsets in patients with stable coronary artery disease. J Clin Lipidol 2021;15:512-521.
29. Williams EL, Stimpson ML, Lait PJP, et al. Glucocorticoid treatment in patients with newly diagnosed immune thrombocytopenia switches CD14(++) CD16(+) intermediate monocytes from a pro-inflammatory to an anti-inflammatory phenotype. Br J Haematol 2021;192:375-384.
30. Graff RM, Kunz HE, Agha NH, et al. beta(2)-Adrenergic receptor signaling mediates the preferential mobilization of differentiated subsets of CD8+ T-cells, NK-cells and non-classical monocytes in response to acute exercise in humans. Brain Behav Immun 2018;74:143-153.
31. Rutkowska-Zapała M, Suski M, Szatanek R, et al. Human monocyte subsets exhibit divergent angiotensin I-converting activity. Clin Exp Immunol 2015;181:126-32.
32. Thaler B, Hohensinner PJ, Krychtiuk KA, et al. Differential in vivo activation of monocyte subsets during low-grade inflammation through experimental endotoxemia in humans. Sci Rep 2016;6:30162.

Table 1: Correlation of different monocyte subsets to CAD and outcomes

Investigators	Subjects (n)	Condition	Target measure	Main outcome
Shantsila et al.	245	STEMI	IMD	↑MACE
Abo-Aly et al.	100	STEMI	IMD	↑MACE
Boidin et al.	245	STEMI	IMD	↑MACE, ↓LVEF
Foster et al.	18	STEMI	$CD11c^+$ IMD	↑troponin, ↑CK, ↑plaque necrosis
Yamamoto et al.	50	stable CAD	IMD	↓fibrous cap thickness
Arnold et al.	40	stable CAD	IMD, NCM	↑CAD severity
Merinopoulos et al.	30	elective PCI	IMD	↑chronic post PCI
Rogacev et al.	951	elective PCI	IMD	↑MACE
Lo et al.	588	asymptomatic	IMD	↑plaque score, ↑coronary stenosis
Markofski et al.	45	older adults	TLR^+ CM, $CD16^+$	↑cardiometabolic risk

CAD, coronary artery disease; CK, creatine kinase; CM, classical monocytes; IMD, intermediate monocytes; LVEF, left ventricular ejection fraction; MACE, major adverse cardiovascular events; NCM, nonclassical monocytes; PCI, percutaneous coronary intervention; STEMI, ST-elevation myocardial infarction; TLR, toll-like receptor

Table 2: The magnitude of the effects of different treatments on monocyte subsets

Investigators	Subjects (n)	Condition	Treatment	Main outcome
Krychtiuk et al.	69	stable CAD	statin	↑PCSK9, ↑CM, ↓NCM
Williams et al.	11	immune thrombocytopenia	prednisolone	↓IMD
Graff et al.	14	exercise	nadolol	↓NCM
Rutkowska-Zapała et al.	4-12	healthy donors	no	↑Ang II, ↑ACE1/2 in CM
Thaler et al.	12	low-grade inflammation	LPS	↑IL-6/8 in IMD and NCM

ACE, angiotensin-converting enzyme; Ang, angiotensin; CAD, coronary artery disease; CM, classical monocytes; IL, interleukin; IMD, intermediate monocytes; LPS, lipopolysaccharide; NCM, nonclassical monocytes.

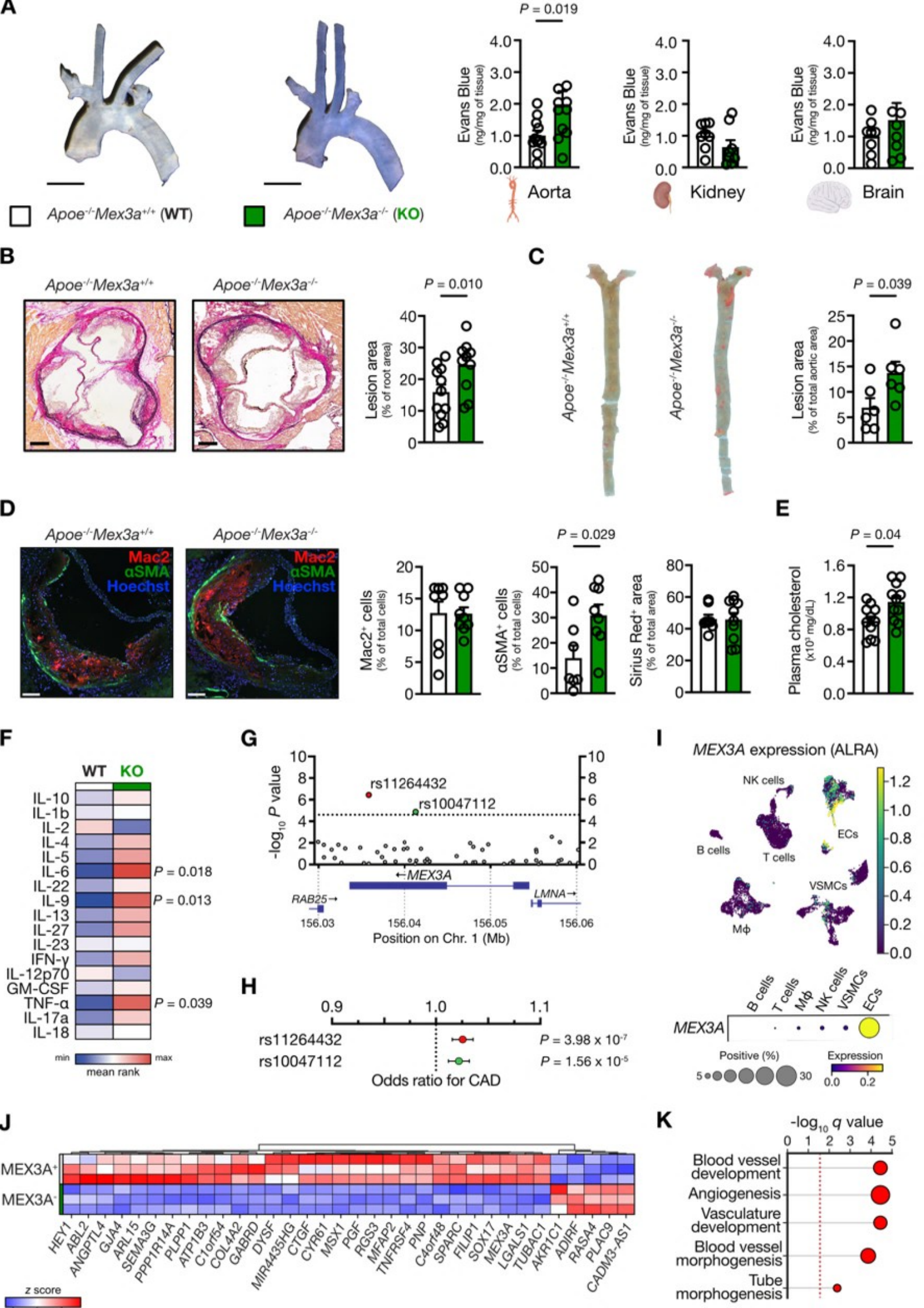
A
P = 0.019
Evans Blue (ng/mg of tissue)
Aorta
Kidney
Brain
Apoe-/-Mex3a+/+ (WT)
Apoe-/-Mex3a-/- (KO)
B
Apoe-/-Mex3a+/+
Apoe-/-Mex3a-/-
P = 0.010
Lesion area (% of root area)
C
P = 0.039
Lesion area (% of total aortic area)
D
Mac2
αSMA
Hoechst
P = 0.029
Mac2+ cells (% of total cells)
αSMA+ cells (% of total cells)
Sirius Red+ area (% of total area)
E
P = 0.04
Plasma cholesterol (x10³ mg/dL)
F
WT
KO
IL-10
IL-1b
IL-2
IL-4
IL-5
IL-6
IL-22
IL-9
IL-13
IL-27
IL-23
IFN-γ
IL-12p70
GM-CSF
TNF-α
IL-17a
IL-18
P = 0.018
P = 0.013
P = 0.039
min
max
mean rank
G
-log10 P value
rs11264432
rs10047112
←MEX3A
RAB25→
LMNA→
Position on Chr. 1 (Mb)
H
rs11264432
rs10047112
P = 3.98 x 10-7
P = 1.56 x 10-5
Odds ratio for CAD
I
MEX3A expression (ALRA)
NK cells
B cells
T cells
ECs
VSMCs
Mϕ
MEX3A
Positive (%)
Expression
J
MEX3A+
MEX3A-
HEY1
ABL2
ANGPTL4
GJA4
ARL15
SEMA3G
PPP1R14A
PLPP1
ATP1B3
C1orf54
COL4A2
GABRD
DYSF
MIR4435HG
CTGF
CYR61
MSX1
PGF
RGS3
MFAP2
TNFRSF4
PNP
C4orf48
SPARC
FILIP1
SOX17
MEX3A
LGALS1
TUBAC1
AKR1C1
ADIRF
RASA4
PLAC9
CADM3-AS1
z score
K
-log10 q value
Blood vessel development
Angiogenesis
Vasculature development
Blood vessel morphogenesis
Tube morphogenesis